MASTER OF PHILOSOPHY Modelling of Materials

Examiners' Solutions to Paper 1

SECTION A

1(a)

A Bravais lattice is an infinitely repeating set of points related by translational symmetry, i.e. each lattice point has an identical environment. The motif is the element of structure associated with each lattice point. The conventional unit cell is oriented in a specific way to the symmetry elements of a crystal, and may or may not be primitive.

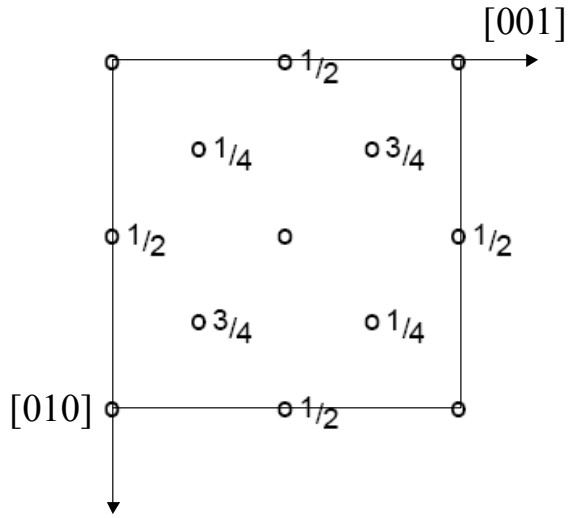

Projection of diamond structure onto (100)

Rotational symmetry about [100] axis through carbons is of order 2 (diad).

1(b)

The embedded atom model is an empirical implementation of effective medium theory.

The total energy of a metal is written as the sum of two terms:

$$U_{tot} = U_A + U_R$$

where U_A = the energy (attractive) required to embed an atom into the density ρ of the neighbouring atoms where ρ is taken to be the superposition of *atomic* charge densities ρ^A

$$U_A = \sum_i F(\rho_i), \qquad \rho_i = \sum_{ij} \rho^A(r_{ij})$$

and U_R = the repulsive overlap energy between atom cores (taken to be a pair potential)

$$U_R = \frac{1}{2} \sum_{ij} \phi(r_{ij})$$

The exact form of $F(\rho_i)$ is not known but various functions such as power laws and exponentials are used. It is fitted to match the bulk properties of the metal (lattice parameters etc).

In general $F(\rho_i)$ is a non-linear function of ρ and is concave negative.

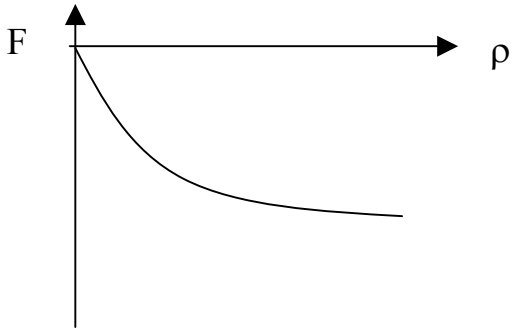

This shape reflects the fact that the energy/atom in a crystal decreases non-linearly with increasing co-ordination Z

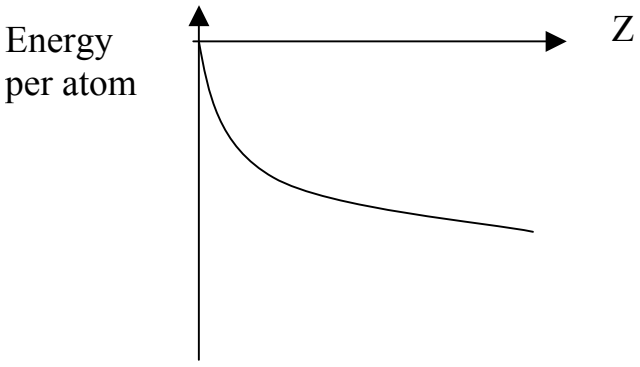

In fact tight-binding theory predicts that the energy/atom is proportional to $-\sqrt{Z}$. Finnis and Sinclair used this result in their formulation of the embedded atom method by requiring $F(\rho_i)$ to have a square root form.

1(c)

The distinction between deterministic and stochastic models is based on whether they are probabilistic in nature or not. Deterministic models use algebraic or differential equations to model system evolution in an unambiguous and reproducible manner. In other words the system outputs are causally connected to the system inputs. Molecular dynamics is given as an example. In some cases, deterministic models can be unpredictable. This may happen if the system dynamics is nonlinear, if a large number of inputs are needed, if the inputs are needed with unrealistically high precision and if the model's stability depends on intermediate calculations. For example, weather forecasting is in principle deterministic but unpredictable in practice. Stochastic models incorporate probabilistic steps, especially in the way structures evolve. They were originally designed to simulate canonical ensembles by performing a large number of iterative steps using random numbers. Monte Carlo is given as an example. In this method the system evolves via a statistical sampling process following a Boltzmann distribution. A given configuration depends only on the previous configuration in the sequence. When the outcome of a random event depends only on the outcome of a immediately previous event, the sequence of structures generated is called a Markov chain. In this sense the method is unpredictable but it is known that average properties generated by deterministic and stochastic models should be same (Ergodic hypothesis). Some models are hybrid in character, having both deterministic and stochastic features (e.g. Brownian dynamics).

1(d)

"Eco selection" is systematic procedure for selecting materials to minimise environmental burden caused by engineering applications, taking in to account the production, the use and the disposal phases. Legislation on the need to disclose the use of energy and CO_2 emissions for manufactured items is increasing. The expenditure of energy can be modelled by considering four major steps:

(i) material production;

(ii) object manufacture and delivery;

(iii) object usage;

(iv) object disposal (including recycling).

By understanding where energy is expended, it then is possible to refine the manufacturing of objects to reduce its usage and, similarly, CO_2 emissions.

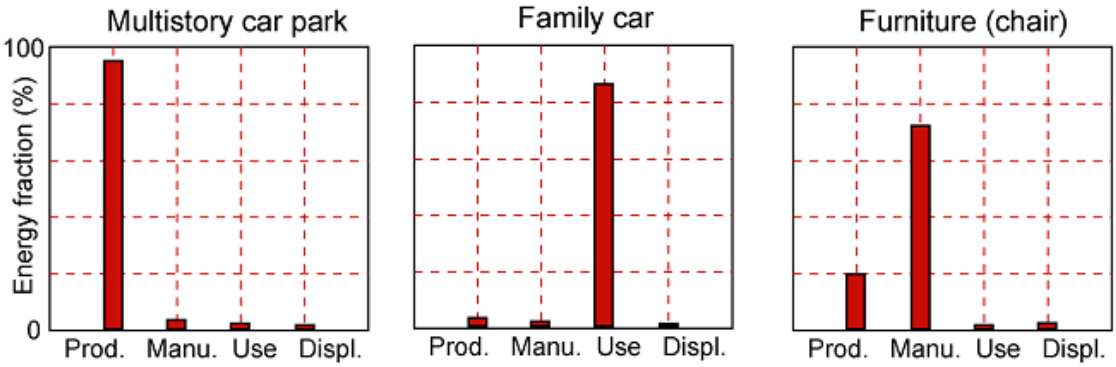

Students expected to comment on the need then to target specific steps in order to improve energy accountability.

1(e)

```
      real function det (a)
      implicit none
      real a(2,2), result
      integer epsilon(2,2)
      data epsilon(1,2)/1/
      data epsilon(2,1)/-1/
      data epsilon(1,1), epsilon(2,2) /0, 0/
      integer i,j
      result = 0.0
      do 10, i = 1, 2
        do 10, j = 1, 2
          result = result + real (epsilon(i,j)) * a(1,i) * a(2,j)
10    continue
      det = result
      return
      end
```

It would be much faster and clearer in practice to return the value

```
a(1,1) * a(2,2) - a(1,2) * a(2,1)
```

1(f)

Quantum mechanical tunnelling is when a particle passes through a region where the potential energy $V > E$, i.e. a region which would be forbidden classically. The answer should include a *brief* discussion of two of the following:

(i) alpha-particle decay

(ii) field emission

(iii) scanning tunnelling microscopy (STM)

1(g)

Thermal importance sampling means that the thermodynamic microstates of a system are not sampled uniformly, but with a probability p_i that depends on their Boltzmann factor:

$$p_i = Z^{-1} \exp\left(-\beta \mathrm{E_i}\right)$$

where Z is the partition function defined by $Z = \sum_i \exp\left(-E_i / k_B T\right)$

The idea of thermal importance sampling is crucial to the Metropolis Monte Carlo method, which is designed to generate states with a frequency that exactly corresponds to their thermal 'importance', defined by p_i above. Thus, the thermodynamic averages of mechanical quantities Q (such as internal energy, volume, pressure) can be computed as an arithmetic average over sampled states.

$$\langle Q \rangle = \frac{1}{M} \sum_{i=1}^{M} Q_i$$

1(h)

Diffusive behaviour will occur on the mesoscale where the microscopic degrees of freedom relating to atomistic motions are thermally equilibrated and give rise to a dissipative frictional force and a fluctuating (Langevin) force on larger particles, which act to produce random walk motion (i.e. mean-square displacement proportional to square root of time, or number of steps). The Langevin force does not conserve momentum between microscopic collisions and mesoscopic motion, although its time-averaged value is zero. The crucial difference between this and systems showing hydrodynamic behaviour is that momentum is strictly conserved in each collision between the fluid particles and the mesoscopic particle. This has observable consequences in polymeric systems, for example the Rouse model for short chains in the melt state predicts a diffusion coefficient which is proportional to N^{-1} (diffusive) whereas the Zimm model for chains in solution predicts a $N^{-0.6}$ dependence (hydrodynamic).

1(i)

Material properties of the GaAs-AlGaAs layers confine the electrons to a thin layer (~ 10 nm). Momentum perpendicular to this layer is quantised.

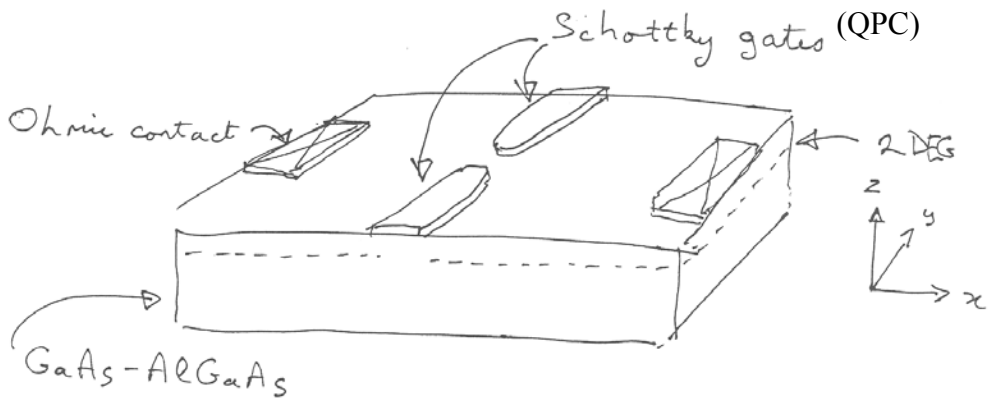

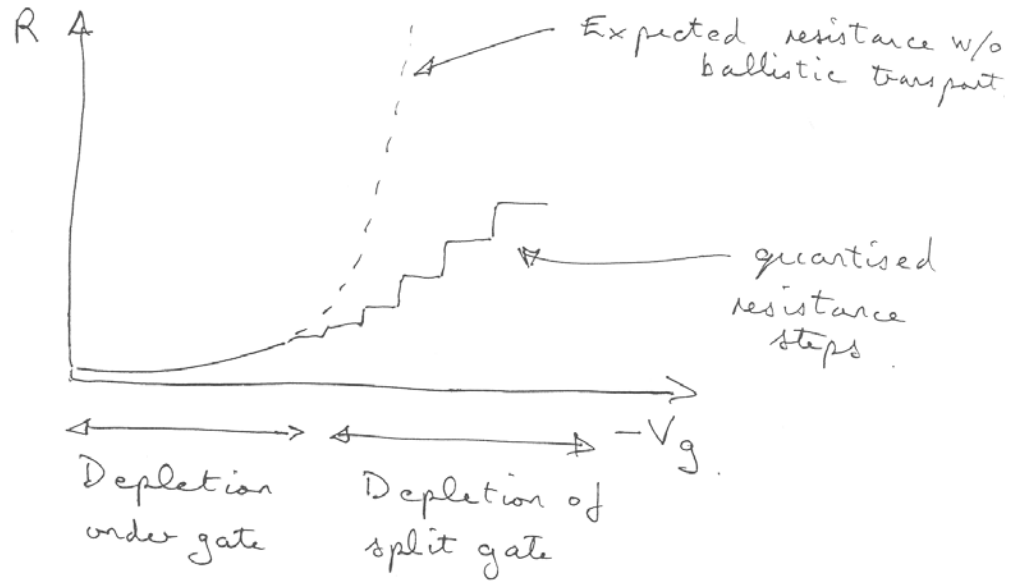

Similarly, electrons are confined in the plane of the 2DEG by the gates (but the well width now depends on the gate voltage). Transmission through split gate is ballistic (at low temperature) so that there is no scattering resistance. Resistance is due to contact between 2DEG and QPC (quantum point contact). Each available energy level gives rise to a separate channel for the transmission of electrons. Total conductance of QPC is:

$$G = \frac{2e^2}{h}\sum_n T_n$$

Transmission of channel n is $T_n = 1$ for no scattering and $h/2e^2$ is the resistance quantum, which is highest resistance possible for open QPC.

1(j)

If $\varepsilon_2 = \varepsilon_3 = 0$, it follows that from Hooke's law in 3D that:

$$\varepsilon_2 = 0 = \frac{1}{E}\left(\sigma_2 - \nu(\sigma_3 + \sigma_1)\right)$$
$$\varepsilon_3 = 0 = \frac{1}{E}\left(\sigma_3 - \nu(\sigma_1 + \sigma_2)\right)$$

Hence if we subtract the second of these equations from the first we find:

$$0 = \frac{1}{E}(\sigma_2 - \sigma_3)(1 + \nu)$$

Since neither $1/E$ nor $(1+\nu)$ will be zero for the general situation, we find $\sigma_2 = \sigma_3$, as we would expect from symmetry.

Substituting this condition back into the equation for ε_2, we find:

$$\sigma_2 = \sigma_3 = \frac{\nu\sigma_1}{(1-\nu)}$$

and so in the '1' direction we have:

$$\varepsilon_1 = \frac{1}{E}\left(\sigma_1 - \nu(\sigma_2 + \sigma_3)\right) = \frac{\sigma_1}{E}\left(1 - \frac{2\nu^2}{1-\nu}\right) = \frac{\sigma_1}{E}\left(\frac{1-\nu-2\nu^2}{1-\nu}\right)$$

Therefore, the 'effective modulus' σ_1/ε_1 is simply:

$$\frac{\sigma_1}{\varepsilon_1} = \frac{E(1-\nu)}{1-\nu-2\nu^2}$$

For a material whose Poisson's ratio is ≈ 0.5 the term $1-\nu-2\nu^2$ approaches zero, so the material becomes very stiff in the above constraint situation

[The marked increase in stiffness in this constraint situation occurs in rubber, which has a Poisson's ratio of ≈ 0.5. For small values of ν (e.g., $\nu < 0.1$) the difference between the above expression and E is negligible.]

SECTION B

2.

The following table summarises the comparison between neural networks and polynomial regression techniques.

Neural networks	**Polynomial regression**
Adaptive functions (shape not determined by user)	Shape pre-determined
Can cope with very complex variations	Complexity limited to choice of function
Can cope with interactions between input parameters	Can only take into account interactions inasmuch as they are deliberately introduced in the function chosen
Problems associated with NN are overfitting and the need for an indication of the uncertainty of fitting. The former occurs as a result of the flexibility of the functions defined by complex NNs. The latter is a consequence of the typical problems treated in NN, which are often complex and involve thousands of data points. As a result, it is difficult for the user to have an idea of where data points may be lacking to obtain a suitable model. To be of practical use, the model must therefore be able to communicate a prediction and an 'error bar' which represent the uncertainty of fitting. In regions with little data, the uncertainty of fitting will be large and user should consider predictions with caution.	Overfitting is inherently impossible as the function is not adaptable. Because the problems treated with 'classical' regression methods are typically simpler, there is perhaps no need for a method to estimate the uncertainty of fitting.
In practice, the method is computer intensive and requires highly specialised software. A computer is also required to make predictions and the model must be distributed.	These 'models' are very easily communicated (in written form typically) and can be used at most levels of skills in the industry. They do not require highly specialised software.

The 'meaning' of the model can only be examined by making predictions.	The 'meaning ' of the model is directly visible, (e.g strength = 430 + 200C + 50Cr indicates a stronger effect of C on strength).

[35%]

One risk with NN is overfitting. This occurs when noise rather than the general trend is fitted during the regression and is possible when using NN because of the flexibility of the typical networks used. A first way to avoid this is to use a regulariser, which penalises large values of weights (adjustable parameters). Large values of weights are associated with sharp variations while small values are associated with smooth variations. The students may also describe this in terms of prior belief and penaliser/regulariser alpha (large values of alpha penalises strongly large values of weights => correspond to the belief that the fitting function should be smooth). A second method is to divide the database in two sets. The first set is used to optimise the adjustable parameters, the second to verify that no overfitting has occurred. A drawing may be included here.

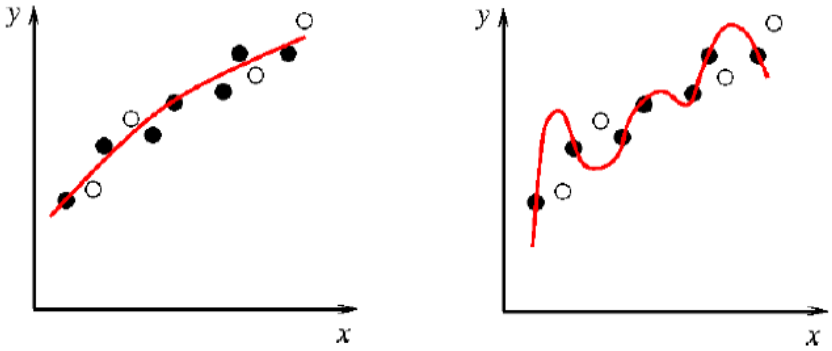

Another difficulty lies in the problem of assessing the quality of the output. Although this is not intrinsic to NN, the fact that they are mostly used for complex problems makes this issue more relevant: with large number of input variables, it is frequently the case that some regions of the input space contain very little information. In these areas, the fitting is uncertain and we need to communicate this as well as the fitting itself.

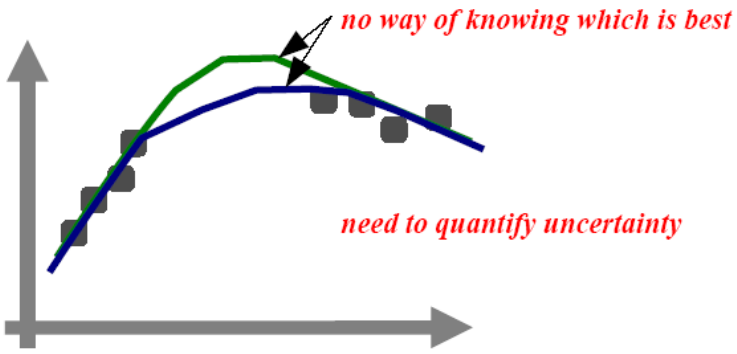

Conventional approach (error function minimisation to identify optimum parameters) cannot include this uncertainty. The Bayesian approach solves this by optimising a probability distribution on the parameters rather than identifying a single set of parameters. Where this probability distribution is 'wide', the uncertainty is large.

[35%]

The answer should include the following points:

- A discussion on the size of the database used in comparison with the number of adjustable parameters in the chosen neural network structure. This should be deduced from the number of input variables (5+bias=6) and the structure of the network (3HU therefore 3*6+4=22 adjustable parameters). It is typically recommended to have 5-10 input data per adjustable parameter. Therefore, the database was not suitable by far.
- It may also indicate that there is no indication why such a structure was chosen, it is best to explore a variety of structures and rank them.
- The text indicates that the 15 data points were collected and used to train the model. The comparison made after training is therefore on data used for the training and is entirely meaningless. It is likely that overfitting occurred.

The conclusion is obviously that rejection is justified.

[30%]

3.

(a) The Jominy end-quench test is used to measure the hardenability of steels. It produces a continuous variation of cooling rate along the bar. The cooling rate governs the phases formed from austenite, notably the formation of martensite when diffusion-controlled transformations are avoided (above the critical cooling rate). This is detected by hardness testing along the bar.

[10%]

(b)

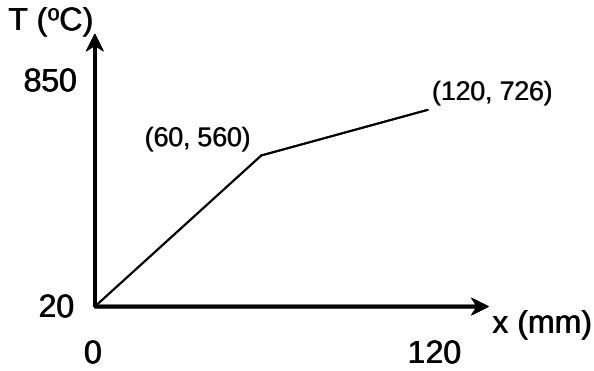

Key points:
- straight lines between nodes
- temperature at x = 0 is 20°C

[20%]

(c) (i)

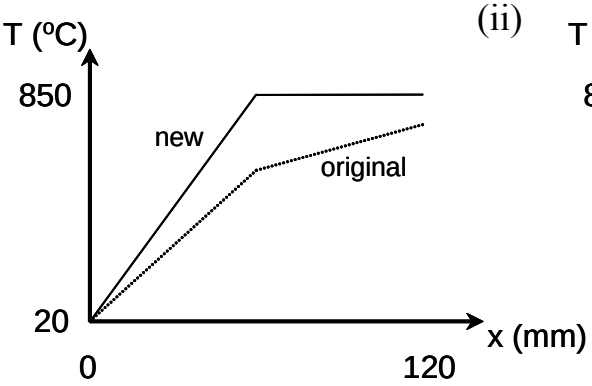

Key points:
- straight lines between nodes
- in 1 second, temperature effectively unchanged from initial value at nodes 2 or 3

(ii)

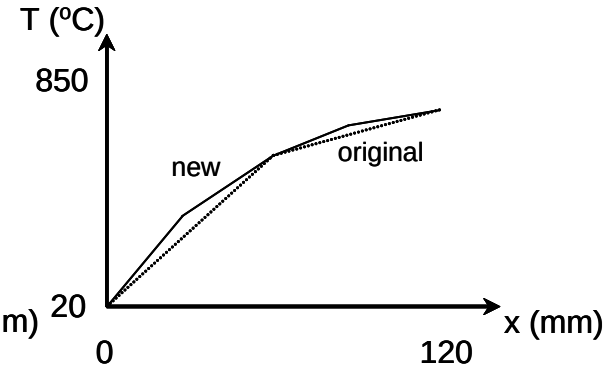

Key points:
- straight lines between nodes
- predicted temperatures unchanged at x = 0, 60, 120 mm

(iii)

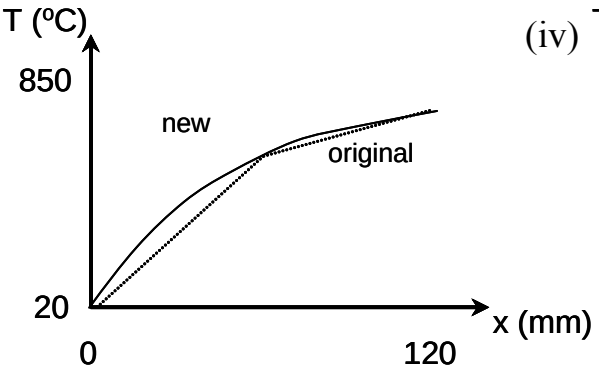

(iv)

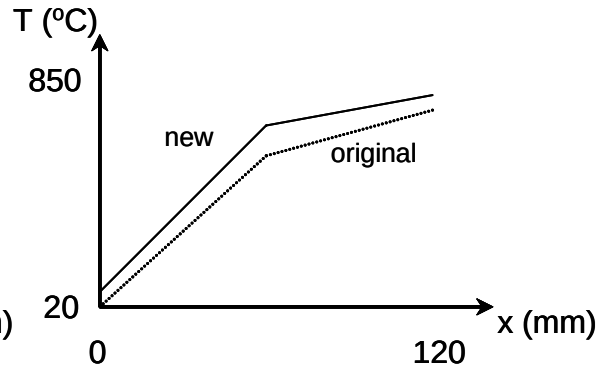

Key points:
- new model smoothly curved between nodes
- predicted temperatures unchanged at x = 0, 60, 120 mm

Key points:
- straight lines between nodes
- temperature still above 20 at x = 0, and also higher at nodes 2 and 3

[40%]

(d) The analytical solution assumes a semi-infinite bar, but the other conditions are identical. The predicted temperature is evaluated continuously in *x*, rather than being interpolated between nodal values.

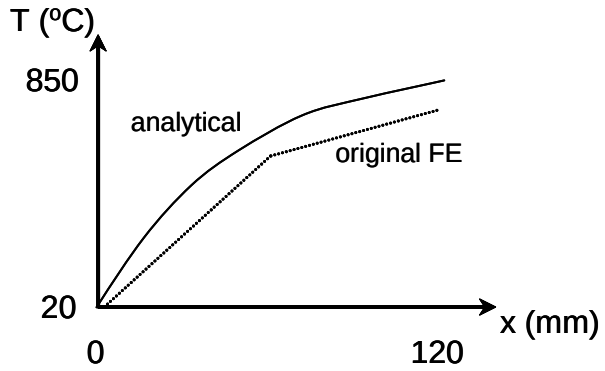

Key points:
- analytical model smoothly curved, gradient zero at unquenched end.
- analytical solution higher than FE, because FE model has a finite length, so no heat is conducted into the bar at x = 120mm; the analytical model is semi-infinite, so heat continues to be conducted in from the far field (x > 120

[30%]

4.

From the formula given in the question, it is apparent that the deformation tensor e_{ij} takes the form:

$$e_{ij} = \gamma \begin{pmatrix} n_1\beta_1 & n_2\beta_1 & n_3\beta_1 \\ n_1\beta_2 & n_2\beta_2 & n_3\beta_2 \\ n_1\beta_3 & n_2\beta_3 & n_3\beta_3 \end{pmatrix}$$

where the components of **n** and **β** are defined in a reference set of orthonormal axes.

This deformation tensor can be separated into a symmetric strain tensor ε_{ij} and an anti-symmetric rotation tensor ω_{ij}. The symmetric strain tensor ε_{ij} is clearly:

$$\varepsilon_{ij} = \gamma \begin{pmatrix} n_1\beta_1 & \frac{1}{2}(n_2\beta_1 + n_1\beta_2) & \frac{1}{2}(n_3\beta_1 + n_1\beta_3) \\ \frac{1}{2}(n_1\beta_2 + n_2\beta_1) & n_2\beta_2 & \frac{1}{2}(n_3\beta_2 + n_2\beta_3) \\ \frac{1}{2}(n_1\beta_3 + n_3\beta_1) & \frac{1}{2}(n_2\beta_3 + n_3\beta_2) & n_3\beta_3 \end{pmatrix}$$

This tensor has to be symmetric so that the strain produces normal strain and shear strains without any rotation.

[20%]

The trace of this matrix is simply:

$$\gamma\left(n_1\beta_1 + n_2\beta_2 + n_3\beta_3\right) = \gamma\mathbf{n}.\boldsymbol{\beta} = 0$$

since, by definition, the slip plane must contain the slip direction, so that the scalar product of **n** and **β** is zero. [10%]

In lithium fluoride there are six distinct planes of the type {110}. Within each plane there is only one distinct $<1\bar{1}0>$ direction. Hence, there are six physically distinct slip systems.

[10%]

Slip systems which produce different pure strains are said to be independent. Thus, we need to evaluate the strain tensors for each of these six physically distinct slip systems.

It is convenient to label the six slip systems A – F for simplicity:

Label	Slip system
A	$(110)[1\bar{1}0]$
B	$(1\bar{1}0)[110]$
C	$(011)[01\bar{1}]$

Label	Slip system
D	$(01\bar{1})[011]$
E	$(101)[10\bar{1}]$
F	$(10\bar{1})[101]$

Looking at slip system A, the strain tensor produced by shearing an angle γ is:

$$\boldsymbol{\varepsilon}_{\mathrm{A}} = \frac{\gamma}{2}\begin{pmatrix} 1 & 0 & 0 \\ 0 & -1 & 0 \\ 0 & 0 & 0 \end{pmatrix}$$

since $\mathbf{n} = \left[\frac{1}{\sqrt{2}}, \frac{1}{\sqrt{2}}, 0\right]$ and $\boldsymbol{\beta} = \left[\frac{1}{\sqrt{2}}, -\frac{1}{\sqrt{2}}, 0\right]$ (choosing our orthonormal set of axes to be parallel to the crystal axes).

Evaluating the other five strain tensors in a similar manner, we find:

$$\boldsymbol{\varepsilon}_{\mathrm{B}} = \frac{\gamma}{2}\begin{pmatrix} 1 & 0 & 0 \\ 0 & -1 & 0 \\ 0 & 0 & 0 \end{pmatrix}; \quad \boldsymbol{\varepsilon}_{\mathrm{C}} = \frac{\gamma}{2}\begin{pmatrix} 0 & 0 & 0 \\ 0 & 1 & 0 \\ 0 & 0 & -1 \end{pmatrix};$$

$$\boldsymbol{\varepsilon}_{\mathrm{D}} = \frac{\gamma}{2}\begin{pmatrix} 0 & 0 & 0 \\ 0 & 1 & 0 \\ 0 & 0 & -1 \end{pmatrix}; \quad \boldsymbol{\varepsilon}_{\mathrm{E}} = \frac{\gamma}{2}\begin{pmatrix} 1 & 0 & 0 \\ 0 & 0 & 0 \\ 0 & 0 & -1 \end{pmatrix}; \quad \boldsymbol{\varepsilon}_{\mathrm{F}} = \frac{\gamma}{2}\begin{pmatrix} 1 & 0 & 0 \\ 0 & 0 & 0 \\ 0 & 0 & -1 \end{pmatrix}$$

[30%]

It is immediately apparent that:

$$\boldsymbol{\varepsilon}_{\mathrm{A}} = \boldsymbol{\varepsilon}_{\mathrm{B}}$$
$$\boldsymbol{\varepsilon}_{\mathrm{C}} = \boldsymbol{\varepsilon}_{\mathrm{D}}$$
$$\boldsymbol{\varepsilon}_{\mathrm{E}} = \boldsymbol{\varepsilon}_{\mathrm{F}}$$

so that there are at most three independent slip systems. However, an examination of $\boldsymbol{\varepsilon}_{\mathrm{E}}$ shows that it can be produced by a linear combination of $\boldsymbol{\varepsilon}_{\mathrm{A}}$ and $\boldsymbol{\varepsilon}_{\mathrm{C}}$:

$$\boldsymbol{\varepsilon}_{\mathrm{E}} = \boldsymbol{\varepsilon}_{\mathrm{A}} + \boldsymbol{\varepsilon}_{\mathrm{C}}$$

i.e., in words, shear of an amount γ on the slip system $(110)[1\bar{1}0]$ combined with shear of the same amount γ on $(011)[0\bar{1}1]$ together produce a shape strain equivalent to shear of an amount γ on the slip system $(101)[10\bar{1}]$. Hence there are only two independent slip systems in lithium fluoride, e.g., $\boldsymbol{\varepsilon}_{\mathrm{A}}$ and $\boldsymbol{\varepsilon}_{\mathrm{C}}$.

[15%]

For a material to be able to deform plastically in response to a general system of stresses, there have to be five independent slip systems to be able to generate the five independent components of the strain matrix in a plastic strain deformation situation (the trace of the strain matrix has to be zero in plastic deformation since volume is conserved – this reduces the number of independent components from six to five).

Lithium fluoride has only two independent slip systems. Hence, we can infer that it will not be ductile in a general loading situation. Instead, it will fracture.

[15%]

5.

The average internal energy of the system in thermal equilibrium can be computed from the partition function $Z = \sum_i \exp\left(-E_i / k_{\mathrm{B}}T\right)$, or alternatively $Z = \sum_i \exp\left(-\beta E_i\right)$, where $\beta = 1/(k_{\mathrm{B}}T)$ and E_i are the energies of each microstate i. In each case, the sum runs over all microstates of system, so account must be taken of the degeneracies of each macrostate.

For a single particle: $Z_1 = 1 + 3\exp(-\beta\varepsilon) + 5\exp(-2\beta\varepsilon)$

Hence, $\langle U \rangle = -\frac{1}{Z_1}\frac{\partial Z_1}{\partial \beta} = \frac{3\varepsilon\exp\left(-\beta\varepsilon\right) + 10\varepsilon\exp\left(-2\beta\varepsilon\right)}{1 + 3\exp\left(-\beta\varepsilon\right) + 5\exp\left(-2\beta\varepsilon\right)}$

When $T = \varepsilon / k_{\mathrm{B}}$, then $\beta = 1/\varepsilon$, and hence $\langle U \rangle = \frac{3\varepsilon\exp(-1) + 10\varepsilon\exp(-2)}{1 + 3\exp(-1) + 5\exp(-2)}$

[30%]

$$C_V = \frac{\partial U}{\partial T} = \frac{\partial U}{\partial \beta}\frac{\partial \beta}{\partial T}$$

Hence,

$$C_V = \frac{1}{k_B T^2}\left\{\begin{array}{c}\dfrac{\left(-3\varepsilon\exp\left(-\beta\varepsilon\right)-10\varepsilon\exp\left(-2\beta\varepsilon\right)\right)\left(3\varepsilon\exp\left(-\beta\varepsilon\right)+10\varepsilon\exp\left(-2\beta\varepsilon\right)\right)}{\left(1+3\exp(-\beta\varepsilon)+5\exp(-2\beta\varepsilon)\right)^2} \\ +\dfrac{3\varepsilon^2\exp\left(-\beta\varepsilon\right)+20\varepsilon^2\exp\left(-2\beta\varepsilon\right)}{1+3\exp(-\beta\varepsilon)+5\exp(-2\beta\varepsilon)}\end{array}\right\}$$

In the limit when T becomes large, then $\exp(-\beta\varepsilon) \to 1$, and hence:

$$C_V = \frac{1}{k_B T^2}\left\{\frac{\left(-3\varepsilon-10\varepsilon\right)\left(3\varepsilon+10\varepsilon\right)}{81}+\frac{23\varepsilon^2}{9}\right\} = \frac{38}{81}\frac{\varepsilon^2}{k_B T^2}$$

[50%]

If particles are not independent, then partition function will not factorise and the analytical derivative of the internal energy will become extremely unwieldy to compute. An alternative is to use Metropolis Monte Carlo (constant volume) to calculate the system energy. A brief summary of the general Monte Carlo algorithm should be given.

[20%]

6.

The four fabrication steps are described by following diagrams.

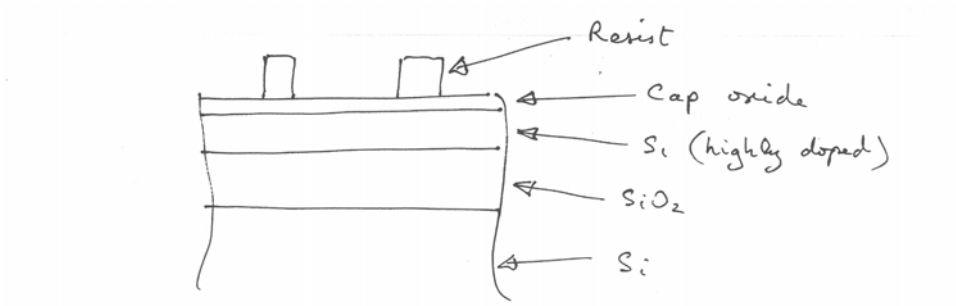

I E-beam lithography. Feature size <100nm

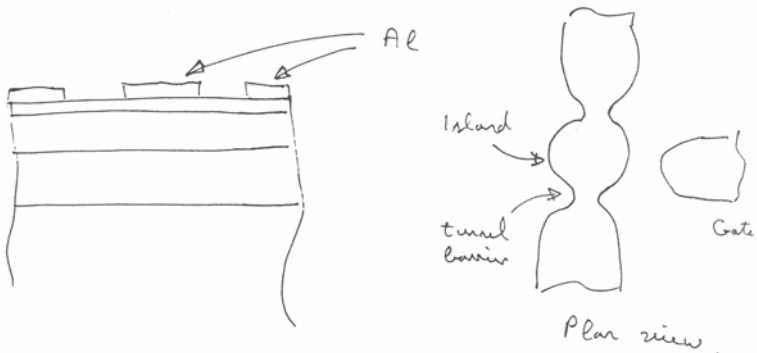

II Al lift-off (Removable mask)

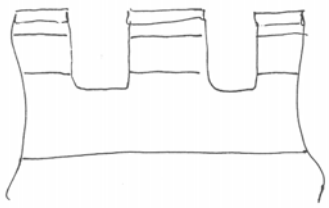

RIE reactive ion etch.

III RIE etch (Anisotropic etch to underlying SiO_2 layer)

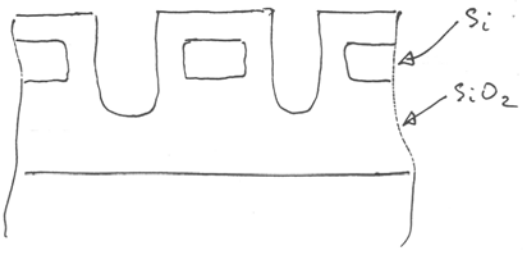

IV Thermal oxidation (Passivation of surface states)

[20%]

(a)

Coulomb blockade involves a small island of charge situated between two electrodes. If the island is small enough and has N electrons then an energy gap opens up between the energy of the last (Nth) electron and the first empty electron state (N+1)th. The size of the gap is equal the square of the electron charge e^2 divided by the capacitance of the island C. Therefore if the island is small enough so that this energy gap is larger than the thermal energy of the system (k_BT), then electrons cannot quantum mechanically tunnel through the system, since the only free states that electrons may tunnel onto the island are above the energy of the electrons in the electrodes. If, however, a gate is used to electrostatically move the island's energy states with respect to the electrodes then the (N+1)th electron free state can be moved below that of one of the electrodes and electrons can quantum mechanically tunnel through the island, one at a time, effectively giving rise to a single electron transistor. Therefore the current-voltage characteristics have zero current until the applied gate voltage corresponds to $\pm e/2C$ (see figure in part (b) below). The suppression of current at low voltage is called Coulomb blockade and the region below the threshold voltage is called the Coulomb blockade region.

[20%]

(b)

For Coulomb blockade to occur, there are two main conditions that must be met:

(i) The charging energy of the island, E_c, must be greater than k_BT. This can be illustrated by looking at the energy level structure of island.

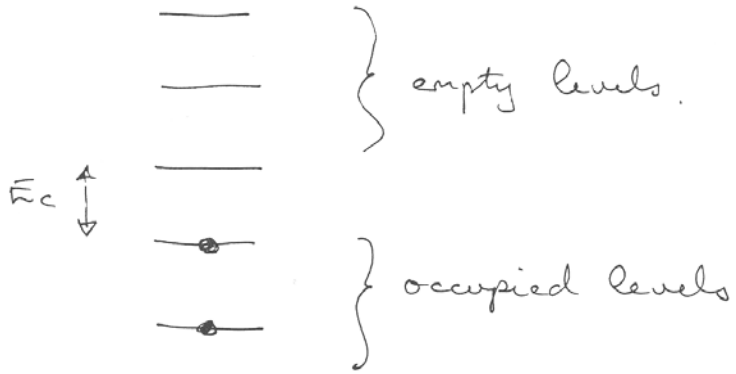

Electrons can only tunnel from lead onto island if there is an available empty energy level. Assuming a metallic lead:

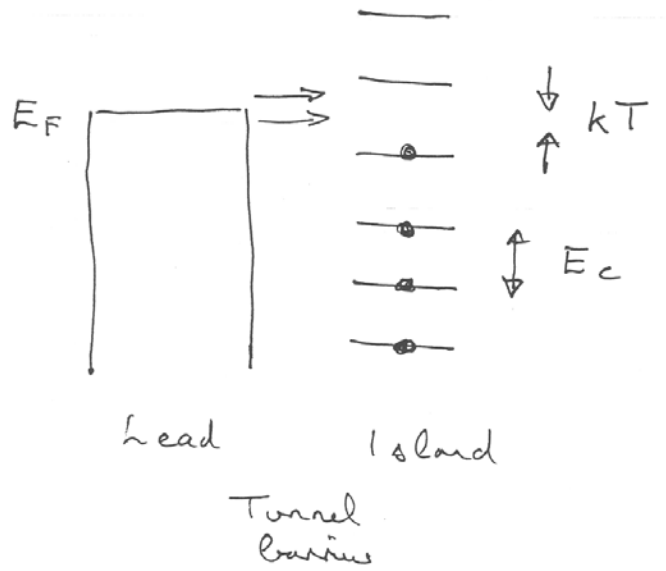

Electrons available for tunnelling from a range of energies of width k_BT around the Fermi energy in the lead. Clearly, if $k_BT < E_c$, then at least one energy level will be available at all times.

Tunnel barrier resistance must be much larger than the resistance quantum h/e^2. The location of the electron is described by the spread of the electron wave function. If the tunnel barrier transmission is high (the tunnel barrier resistance equal to one or more open channels $R < h/e^2$) then the electron is not fully contained within the island. Under these conditions, transfer of charge onto the island is not quantised and Coulomb blockade cannot control electron transport.

[20%]

(c) The island capacitance is given by:

$$\begin{aligned} C &= 8\varepsilon_r\varepsilon_0 r \\ &= 8\times 3.9\times 8.8\times 10^{-12}\times 30\times 10^{-9} \\ &= 8.24\times 10^{-18}\ \text{F} \end{aligned}$$

neglecting gate and tunnel barrier capacitance.

The charging energy is given by:

$$E_c = \frac{e^2}{2C}$$
$$= \frac{(1.6\times10^{-19})^2}{2\times8.24\times10^{-18}}$$
$$= 1.55\times10^{-21}\ \text{J}$$

The maximum operating temperature for Coulomb blockade occurs when $E_c = k_B T$. Hence T_{max} given by:

$$T_{max} = \frac{E_c}{k_B}$$
$$= \frac{1.55\times10^{-21}}{1.38\times10^{-23}} = 111\ \text{K}$$

[40%]

7.

The pair potential approximation involves the termination of the many-body expansion of the potential energy at the second term, i.e.:

$$U = \sum_i V_1(r_i) + \sum_{ij} V_2(r_{ij}).$$

In other words, it ignores higher order terms such as the three-body potential. V_2 (the pair potential) is generally dependent only on the distance between two atoms and has no angular dependence.

Range of validity: (a) molecular crystals where atoms have closed-shell configurations similar to atoms (b) ionic crystals where atoms are electrically charged ions and the interaction energy is mainly Coulombic and varies as the inverse of the distance between ions. The pair potential approximation is not valid for covalent materials (directional bonding) or metals (electron density dependent). This is evident from the electron density distributions below where only molecular and ionic crystals have near-spherical shapes indicating that central pair-wise potentials apply.

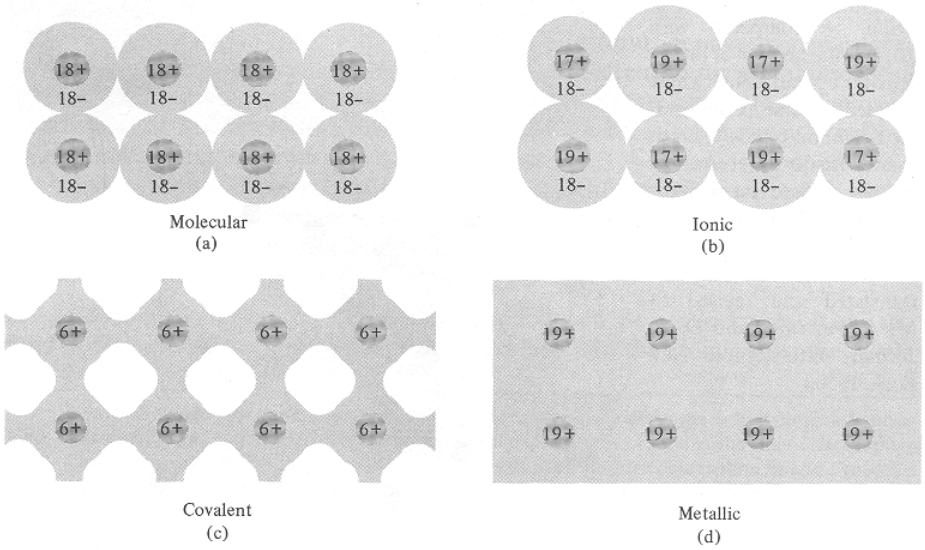

[10%]

(a) The first term is the attraction between atoms. Depending on the material, it can arise from the attraction between ions of opposite sign (ionic bonding), the formation of a molecular orbital (in covalent bonding), the interaction of electric dipoles (van der Waals bonding) and the attraction between molecules that have a permanent dipole moment (hydrogen bonding). The second term comes from the repulsive interaction between overlapping electron shells of neighbouring atoms.

[10%]

(b) The force is given by $\frac{\mathrm{d}U}{\mathrm{d}r} = nAr^{-n-1} - mBr^{-m-1}$

In equilibrium $\frac{dU}{dr} = 0$, and hence $r_0 = \left(\frac{An}{Bm}\right)^{\frac{1}{n-m}}$

The second derivative is given by $\frac{\mathrm{d}^2U}{\mathrm{d}r^2} = -n(n+1)Ar^{-n-2} + m(m+1)Br^{-m-2}$

Therefore:

$$E = \frac{1}{r_0}\frac{\mathrm{d}^2U}{\mathrm{d}r^2}\bigg|_{r_0} = \left(\frac{An}{Bm}\right)^{\frac{-1}{n-m}}\left[-n(n+1)A\left(\frac{An}{Bm}\right)^{\frac{-n-2}{n-m}} + m(m+1)B\left(\frac{An}{Bm}\right)^{\frac{-m-2}{n-m}}\right]$$

$$= \left(\frac{An}{Bm}\right)^{\frac{1}{m-n}}\left[-n(n+1)A\left(\frac{An}{Bm}\right)^{n+2} + m(m+1)B\left(\frac{An}{Bm}\right)^{m+2}\right].$$

For crystal stability $\frac{d^2U}{dr^2} > 0$ at $r = r_0$ (i.e. U must be a minimum)

Therefore: $-n(n+1)Ar_0^{-n-2} + m(m+1)Br_0^{-m-2} > 0$

i.e. $m(m+1)B > n(n+1)Ar_0^{m-n}$

$$m(m+1) > n(n+1)\frac{A}{B}\left(\frac{An}{Bm}\right)^{\frac{m-n}{n-m}}$$

so $m > n$.

[30%]

(c) At the maximum attractive force $\frac{\mathrm{d}^2U}{\mathrm{d}r^2} = 0$.

Therefore $-n(n+1)Ar_f^{-n-2} + m(m+1)Br_f^{-m-2} = 0$

i.e. $r_f = \left(\frac{n(n+1)A}{m(m+1)B}\right)^{\frac{1}{n-m}}$

so $\frac{r_f}{r_0} = \left(\frac{n(n+1)A}{m(m+1)B}\right)^{\frac{1}{n-m}} \left(\frac{An}{Bm}\right)^{\frac{-1}{n-m}} = \left(\frac{n+1}{m+1}\right)^{\frac{1}{n-m}}$.

Sketch of force-distance curve:

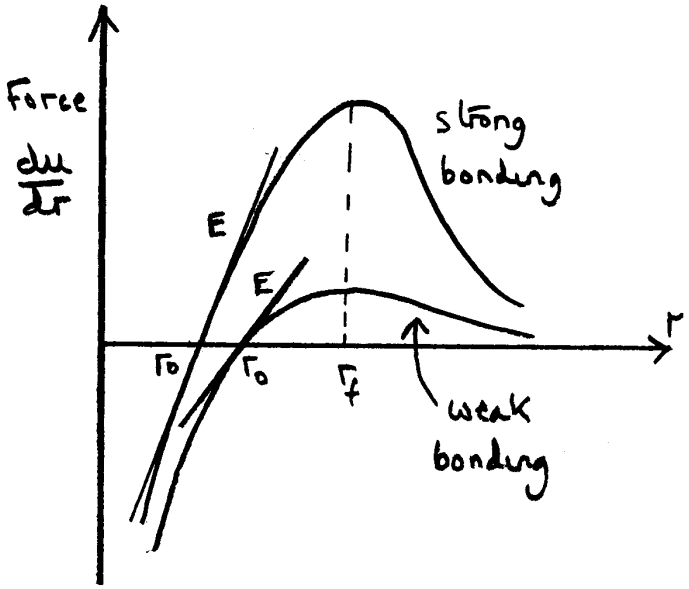

[40%]

(c) For (n, m) = (6, 12) $\frac{r_f}{r_0} = 1.11$ or 11% strain.

For (n, m) = (1, 12) $\frac{r_f}{r_0} = 1.19$ or 19% strain.

The (6,12) potential represents a molecular solid and (1,12) potential represents an ionic solid. So the ionic solid can withstand a greater tensile load before bond breaking occurs, i.e. it has a stronger bond. However, the predicted strains are much different from those actually observed. In ductile materials plastic deformation and the formation of dislocations greatly increases the strain to failure (up to 50%). In brittle materials, the presence of pre-existing flaws and the lack of plastic deformation greatly reduces the strain to failure (down to 2%).

[20%]